Desalination and Water Treatment
www.deswater.com

doi: 10.5004/dwt.2019.24107

159 (2019) 181–192
August

Insight into the removal of Acid Blue 93 by cationic *Eucalyptus* cellulose with different alkyl chain lengths: properties and mechanisms

Fucai Yan, Dongying Hu*

School of Resources, Environment and Materials, Guangxi University, No. 100 Daxue East Road, Nanning 530004, China, emails: hdygxu@163.com (D. Hu), 846920889@qq.com (F. Yan)

Received 20 October 2018; Accepted 8 March 2019

ABSTRACT

Cationized *Eucalyptus* wood chips cellulose (DEC, HEC and OEC) were prepared via grafting with a quaternary ammonium group using *N,N*-dimethyl-1-dodecylamine, *N,N*-dimethyl-1-hexadecylamine or *N,N*-dimethyl-1-octadecylamine as modification agents onto *Eucalyptus* wood chips cellulose (EC) microstructure. The characterization results showed that the molecular structure and morphology of EC changed with the quaternary ammonium group being successfully grafted onto the EC molecular structure. DEC, HEC and OEC with the same degree of substitution were selected as adsorbents for the adsorption of Acid Blue 93 dye to evaluate the dye adsorption performance and mechanism of cationized cellulose with different molecular structures. The adsorption process was well-described by pseudo-second-order and Langmuir models. We found that the adsorption capacity increased with the increasing length of the alkyl chain of the DEC, HEC and OEC. The adsorbents exhibited high reusability and high adsorption performance for dye removal. Thermodynamic parameters indicated that the adsorption process is a spontaneous and feasible process, and that increasing the temperature is conducive to the adsorption process.

Keywords: *Eucalyptus* wood chips cellulose; Modification; Purification; Adsorption mechanism; Non-linear fitting

1. Introduction

Fossil resources play an important role in product manufacture, but they are a limited resource that will eventually run out. A potential solution is to manufacture chemical raw materials from biomass, a renewable resource, rather than petroleum. Lignocellulosic biomass, which is available from forest, agricultural and agro-industrial wastes, has received extensive attention for the preparation of functional materials due to its non-toxic, biodegradable and renewable properties [1]. Plant biomass is the most abundant renewable and biodegradable carbohydrate polymer in nature. In the tropical regions, *Eucalyptus* is a fast-growing hardwood species with good fiber qualities and relatively low market prices [2]. The full utilization of *Eucalyptus* carbohydrates has attracted great interest. In China, the use of *Eucalyptus* is mainly focused on the development of high-performance *Eucalyptus* composite materials, *Eucalyptus* veneer lumber, bamboo raft composites, thick-core *Eucalyptus* solid wood composite panels and aldehyde-free *Eucalyptus* plywood manufacturing technology. *Eucalyptus* brings not only value to the industry, but also economical benefits to other industries. *Eucalyptus* has a complex structure composed mainly of cellulose, lignin and hemicellulose. For the utilization of *Eucalyptus* cellulose, many studies have focused on the use of *Eucalyptus* cellulose in the pulp and paper industry [3], which is accomplished via the extraction of cellulose micro/nanofibers from *Eucalyptus* kraft pulp [4]. By contrast, the main organic components of cellulose from *Eucalyptus* could be utilized in functional materials through purification and modification methods to produce modified cellulose-based materials to expand the potential of *Eucalyptus* for use in materials science [5]. *Eucalyptus* sawdust has potential application value as an industrial residue due

* Corresponding author.

to its specific characteristics, such as high cellulose content, low cost, good biocompatibility and biodegradability [6].

Dyes are widely used in many industrial applications, including textiles, leather, food processing, electroplating, plastics, cosmetics, rubber and printing. More than 100,000 dyes are commercially available. The annual production of these dyes exceeds 70,000 tons, of which about 15%–20% of the dye remains in the wastewater from the dyeing process [7]. The presence of dyes in wastewater is an important environmental issue because of their high visibility, resistance and toxicity [8]. Even low concentrations of dyes can reduce photosynthesis in the aquatic environment by hindering the penetration of light and oxygen [9]. In addition, due to their complex aromatic structure, dyes are non-biodegradable substances that are stable under a variety of conditions; they have direct and indirect toxic effects on humans and are associated with diseases such as cancer, tumors and skin irritation [10]. Therefore, the elimination of dyes from wastewater prior to discharge into the environment is a fundamental priority.

At present, the methods for removing dyes from dye wastewater include flocculation, membrane separation, ion-exchange, photocatalytic oxidation, electrochemical, biochemical and adsorption processes [11]. Among them, adsorption is an important method for dye wastewater treatment, and the choice of adsorbent is the key. The development and utilization of cost-effective, recyclable, and inexpensive adsorbents has become a research hotspot in this field. The adsorption capacity of cellulose has become an area of considerable interest in recent years because it can remove organic pollutants by adsorption, combining low cost and recyclability [12]. Moreover, the ability of cellulose to remove dyes, phenol, and metal ions from wastewater has been demonstrated [13]. However, the adsorption characteristics of natural cellulose are not constant and vary depending on the origin of the cellulose and the initial treatment. The adsorption capacity of the cellulose can be increased by chemical functionalization of the fibers, which can be achieved by introducing chemical groups with high affinity for the chemicals in the aqueous solution.

In the purification of dye wastewater, most of the dyes in water body are positively or negatively charged. The adsorption mechanism is usually caused by electrostatic forces, van der Waals forces, hydrogen bonding and other actions that are induced between the adsorbent and the pollutant molecules [14]. In order to purify the dye wastewater, the adsorbent itself should have a certain charge and a linear structure of the polymer to satisfy the conditions of adsorption neutralization and the adsorption bridging. Cationized or anionized cellulose is a derivative of cellulose, in which cationic or anionic functional groups are grafted onto its active hydroxyl group structure to prepare the appropriate type of modified cellulose. This type of cellulose derivative exhibits cationic or anionic properties at different pH values, which is favorable for the adsorption of anionic or cationic contaminants in water via electrostatic attraction. Moreover, cationized or anionized cellulose is a linear polymer compound that has the potential to form an adsorption bridge action and facilitates the removal of pollutants from the wastewater by adsorption. Because cellulose can be grafted with a cationic or anionic group by chemical modification, it is possible to retain a positively or negatively charged element. However, for different types of dye wastewater, cationized or anionized cellulose has certain specificity for the adsorption particular types of dyes (namely, cationic or anionic dyes). Therefore, cationized cellulose is preferable for removing anionic dyes from dye wastewater.

Quaternary ammonium salts are relatively common cationic-containing compounds that can interact with negatively charged materials on the surface. Surface modification of cellulose with quaternary ammonium salts can be a suitable route for subsequent adsorption of negatively charged contaminants due to the permanent positive charge of quaternary ammonium salts making them efficient anion-exchangers [15]. To date, trimethylamine [16], 3-chloro-2-hydroxypropyltrimethylammonium chloride [17] and tetramethylethylenediamine [18] have been used as modification agents for the preparation of cationic cellulose to purify dye wastewater. A wheat straw-based adsorbent was prepared by a chemical modification method using cetyltrimethylammonium bromide as a modifier and the effect of the adsorbent on the removal of Congo Red dye from wastewater was investigated [19]. The adsorption of Congo Red by derivatized wheat straw was stronger than that of unmodified wheat straw [19]. Cellulose nanofibers (CNF) grafted with glycidyltrimethylammonium chloride (GTMAC), containing quaternary ammonium contents of 0.44 (QCNF-1), 1.47 (QCNF-2) and 2.28 (QCNF-3) mg g^{-1}, were evaluated as flocculants for the removal of reactive orange 16, an anionic azo dye from aqueous solution [20]. We found that there have been many research reports on the preparation of high-performance adsorbent materials using quaternary ammonium salts as cationized agents. However, quaternary ammonium salts with different molecular structures may exhibit differences in properties, resulting in differences in the adsorption capacities of the cationized cellulose prepared by using different quaternary ammonium salts as a modifier, a topic on which there are relatively few relevant reports on the adsorption mechanism of dye wastewater with the different molecular structure characteristic of cationized cellulose.

In this study, *Eucalyptus* wood chips were used as the raw material from which to extract and separate the cellulose contained within the wood chips by alkali or bleaching treatment. The *Eucalyptus* wood chips cellulose was modified with the different molecular structures of *N,N*-dimethyl-1-dodecylamine, *N,N*-dimethyl-1-hexadecylamine or *N,N*-dimethyl-1-octadecylamine as modifying agents to prepare the cationized cellulose. The adsorption properties of the dye Acid Blue 93 onto cationized *Eucalyptus* cellulose were studied. The mechanism of the interaction between the functional groups on the cationized *Eucalyptus* cellulose molecular structure and the groups in the dye molecular structure was discussed. The samples were characterized by the use of Fourier transform infrared spectroscopy (FT-IR), X-ray diffraction (XRD), elemental analysis and scanning electron microscopy (SEM). The adsorption kinetics and equilibrium adsorption behaviors were analyzed to understand the adsorption mechanism. Thermodynamic parameters were also calculated.

2. Experimental setup

2.1. Materials

N,N-dimethyl-1-dodecylamine, *N,N*-dimethyl-1-hexadecylamine and *N,N*-dimethyl-1-octadecylamine was

purchased from Shangdong Banghua Oil Chemical Co., Ltd. (China). Epichlorohydrin, isopropanol, sodium chlorite and other chemical reagents were purchased from Tianjin Kemiou chemical Co., Ltd. in China. Acid Blue 93 was purchased from Sinopharm Chemical Reagent Co., Ltd. (Shanghai, China). All the chemical reagents were directly used without any pretreatment.

2.2. Preparation of cationic Eucalyptus wood chips cellulose

Eucalyptus wood chips used in this work were kindly supplied by Guangxi Hengxian Yachang Wood Processing Factory (Guangxi, China). The wood chips were oven-dried at 110°C for 8 h, following which the dried *Eucalyptus* wood chips were crushed by a grinder and passed through a 30-mesh sieve, and then put into a solution consisting of 40 g L^{-1} of NaOH, 2 g L^{-1} of surfactant, and 2 g L^{-1} of $NaHSO_3$ solution with a bath ratio of 50 g wood chips: 1 L, and stirred at 90°C for 3 h. Next, the chips were washed with plenty of distilled water and dried in a vacuum oven at 60°C. The cellulose obtained was placed into a solution consisting of 10 g L^{-1} of $NaClO_2$, 5 g L^{-1} of acetic acid, and the bath ratio was 35 g: 1 L, with the suspension being stirred at 70°C for 1 h. The upper treatment was repeated three times to obtain pure *Eucalyptus* wood cellulose, which was dried in a vacuum oven at 60°C. Finally, the dried cellulose was ground to a powder and passed through a 40-mesh sieve for further modification processes.

Eucalyptus wood cellulose (EC) powder (10 g) was added to 250 mL of 20% NaOH solution, exposed to ultrasonic radiation at a power of 10.8 kJ g^{-1} for 5 min, and then stirred at room temperature for 30 min to obtain activated *Eucalyptus* wood cellulose. Solid-liquid separation of the sample was then performed. Activated *Eucalyptus* wood cellulose and a solution of NaOH and epichlorohydrin was added into a three-neck round-bottomed flask. The reaction was subsequently stirred at 65°C for 6 h. After filtration, the solution was removed and washed with isopropanol to remove the residual epichlorohydrin. A mixed solution of *N,N*-dimethyl-1-dodecylamine and isopropanol was added to the residue, and the mixture was stirred at 80°C for 3.5 h. The product was filtered and rinsed with a large volume of absolute ethanol to remove the residual *N,N*-dimethyl-1-dodecylamine, followed by 0.1 mol L^{-1} NaOH solution and 0.1 mol L^{-1} HCl solution to adjust solution pH values to around 7, and then washed with a large volume of water to obtain the cationic *Eucalyptus* wood chips cellulose (DEC). DEC was dried in vacuum at 60°C for 10 h. Exploring the influence of the molar ratio of NaOH/*N,N*-dimethyl-1-dodecylamine on the degree of substitution of cationic cellulose (DEC).

Eucalyptus wood cellulose was modified by *N,N*-dimethyl-1-hexadecylamine or *N,N*-dimethyl-1-octadecylamine to obtain the cationic *Eucalyptus* wood chips cellulose (HEC or OEC, respectively), the specific method was as described above.

2.3. Characterization

The nitrogen content (*N*%) of the cationic *Eucalyptus* wood chips cellulose was measured on an elemental analyzer (EA 3000, Arvator, Italy). Fourier-transform infrared spectra (FTIR) of EC, DEC, HEC, OEC were obtained using a Nicolet iS50 spectrophotometer (Thermo Fisher Scientific, USA) in the wavelength range of 4,000~750 cm^{-1} with resolution of 0.09 cm^{-1}. X-ray diffraction (XRD, DX-2700A, Dandong Haoyuan Instrument Co., Ltd. China) analysis was carried out using Cu $K\alpha$ radiation within a 2θ = 5~45° at a scanning rate of 5 min^{-1} at room temperature. The microscopic morphology images of the samples were examined using an S-3400N scanning electron microscope (SEM, Hitachi, Tokyo, Japan).

2.4. Batch adsorption procedure

Adsorption experiments were conducted to test the adsorption performance of DEC, HEC and OEC adsorbents with the same degree of substitution (D_S) for removal of Acid Blue 93 dye from simulated dye wastewater. The effects of different influencing parameters on the adsorption performances were analyzed. Specifically, we studied the adsorbent dosage, contact time, temperatures, initial dye concentration and pH values. After adsorption, the mixture was subjected to centrifugation at 4,000 rpm for 10 min to remove the adsorbent. The residual concentration of Acid Blue 93 after adsorption by adsorbent was measured using an ultraviolet-visible (UV–vis) spectrophotometer (UV-2600, Shimadzu, Kyoto, Japan) at λ_{max} = 570 nm. The removal efficiency, adsorption capacity at equilibrium and at time *t* was calculated using the following equations:

$$R = (C_0 - C_t)/C_0 \times 100\% \quad (1)$$

$$q_e = (C_0 - C_e) \times V/M \quad (2)$$

$$q_t = (C_0 - C_t) \times V/M \quad (3)$$

where C_0, C_e and C_t (mg L^{-1}) are the initial dye concentrations of the solution, the residual solution at equilibrium and at time *t*, respectively. q_e and q_t are the adsorption capacities at time *t* (q_t, mg g^{-1}) and at equilibrium (q_e, mg g^{-1}), respectively. *V* (mL) is the volume of solution and *M* (mg) is the adsorbent dosage.

2.5. Adsorption kinetics and isotherms analysis

The non-linearized kinetics of the adsorption was studied by analyzing the adsorption capacity of Acid Blue 93 onto DEC, HEC and OEC at different time intervals. The adsorption kinetics of the Pseudo-first-order, Pseudo-second-order and Elovich models are given in Table 1 [21].

Adsorption is a complex process composed of many steps, including surface diffusion, intraparticle diffusion and so on. The only use of Pseudo-first-order, Pseudo-second-order and Elovich models does not fully describe the diffusion mechanism in the adsorption process. To more fully analyze the relevant mechanisms of the adsorption process, the intraparticle diffusion model was used to fit the kinetic data [22]. The expression of the intra-particle diffusion model is shown as below:

$$q_t = k_{id} t^{1/2} + c \quad (4)$$

Table 1
Lists of adsorption kinetics and isotherms models

Models		Non-linear form	Plot
Kinetics	Pseudo-first-order	$q_t = q_e(1-e^{-k1t})$	t vs. q_t
	Pseudo-second-order	$q_t = k_2 q_e^2 t/(1 + k_2 q_e t)$	t vs. q_t
	Elovich	$q_t = \ln(1 + \alpha\beta t)/\beta$	t vs. q_t
Isotherms	Langmuir	$q_e = q_m K_a C_e/(1 + K_a C_e)$ $R_L = 1/(1 + K_a C_0)$	C_e vs. q_e
	Freundlich	$q_e = k_f C_e^{1/nf}$	C_e vs. q_e
	Tempkin	$q_e = B\ ln\ A_T C_e$, $B = RT/b_T$	C_e vs. q_e
	Sips	$q_e = q_m K_s C_e^{1/n}/(1 + K_s C_e^{1/n})$	C_e vs. q_e

where c is the intercept (mg g^{-1}) and k_{id} is the intraparticle diffusion rate constant (mg g^{-1} $min^{-1/2}$). These values can be obtained by plotting q_t vs. t.

The non-linearized isotherms of the adsorption at various dye concentrations were analyzed to determine the equilibrium adsorption capacity. The adsorption isotherms of the Langmuir, Freundlich, Tempkin and Sips models are also given in Table 1 [23]. All the data used for the above analysis were the mean values from three replicate tests.

2.6. Thermodynamic analysis

Thermodynamic parameters were calculated from the equilibrium adsorption data at different temperatures. The different thermodynamic parameters can be used to determine the spontaneous, reversible, endothermic or exothermic nature of the adsorption process [24]. The standard Gibbs free energy change ($\Delta G°$), standard enthalpy change ($\Delta H°$) and standard entropy change ($\Delta S°$) can be calculated by using the following equations:

$$\Delta G° = -RT\ln K_d \quad (5)$$

$$K_d = q_e/C_e \quad (6)$$

$$\ln K_d = -\Delta H°/RT + \Delta S°/R \quad (7)$$

where R is the gas constant (8.314 J K^{-1} mol^{-1}), and K_d is the equilibrium constant for the adsorption at standard temperature and pressure. The values of $\Delta H°$ and $\Delta S°$ can be calculated from the slope-intercept of plot between ln K_d vs. $1/T$. All the data used for the above analysis are the mean values from three replicate tests.

2.7. Studies relating to the re-use of the adsorbent

A recyclability experiment was undertaken to test the reusability of the DEC, HEC and OEC adsorbents. After adsorption, the adsorbent was soaked in a 0.1 mol L^{-1} NaOH solution and shaken at 120 rpm for 5 h to obtain the regenerated adsorbent. The regenerated adsorbent was washed with deionized water several times, dried in a vacuum oven at 60°C and weighed for the next reuse cycle. Subsequently, adsorption experiments were carried out to analyze the ability of the regenerated adsorbent to remove Acid Blue 93 dye from the solution. In order to test the reusability of DEC, HEC and OEC adsorbent, the adsorption-desorption cycle was repeated five times.

3. Results and discussion

3.1. Characterization

3.1.1. Elemental analysis

The effect of the molar ratio of NaOH/ *N,N*-dimethyl-1-dodecylamine on the degree of substitution of cationic *Eucalyptus* wood chips cellulose is shown in Table 2. The *D*s values of DEC, HEC and OEC were determined by nitrogen content (*N*%) and calculated according to the following equations [25]:

DEC: $Ds = 162 \times N\%/(14-305.5 \times N\%)$

HEC: $Ds = 162 \times N\%/(14-361.5 \times N\%)$

OEC: $Ds = 162 \times N\%/(14-389.5 \times N\%)$

The *D*s values of DEC, HEC and OEC increased as the molar ratio of NaOH/*N,N*-dimethyl-1-dodecylamine, *N,N*-dimethyl-1-hexadecylamine or *N,N*-dimethyl-1-octadecylamine increased (Table 2). This is because NaOH plays a catalytic role in the etherification reaction. Under the action of NaOH, the epoxy structure grafted onto the molecular structure of the cellulose is opened, promoting the etherification reaction of cellulose and *N,N*-dimethyl-1-dodecylamine, *N,N*-dimethyl-1-hexadecylamine or *N,N*-dimethyl-1-octadecylamine. According to the above *D*s value analysis, the cationic *Eucalyptus* wood chips cellulose (DEC, HEC and OEC) with the same degree of substitution of 0.4 was selected as the adsorbent for the adsorption of Acid Blue 93 dye to evaluate the adsorption performance of cationized cellulose with different molecular structures for dyes, as well as with the respective adsorption mechanisms.

3.1.2. FTIR

The FTIR spectra of EC, DEC, HEC and OEC are shown in Fig. 1(a). For EC, the peaks at 3,329 cm^{-1} are attributed to the O–H stretching vibration of the hydroxyl group. The peak at 2,895 cm^{-1} is attributed to C–H stretching vibration of the $–CH_2–$ groups [26]. A series of peaks at 1,162 cm^{-1}, 1,103 cm^{-1}, 1,030 cm^{-1}, 899 cm^{-1} are attributed to the -COC- group in the

cellulose glucose structure [27]. As can be seen from Fig. 1(a), the spectrum of DEC, HEC and OEC changed slightly compared with that of EC. The O–H stretching vibration band was weaker than that of EC and moved from 3,329 to 3,349, 3,353, 3,357 cm^{-1}. This may be due to the destruction of hydrogen bonds during the modification process. The peak intensity of the -CH_2- group became stronger and a shoulder peak occurred compared with EC. There was a new adsorption peak associated with the stretching vibration of C-N band at 1,457, 1,458, and 1,462 cm^{-1} [28]. All the results indicate that quaternary ammonium salt was successfully grafted onto the EC molecule structure.

3.1.3. XRD

XRD patterns of EC, DEC, HEC and OEC are shown in Fig. 1(b). The XRD pattern of EC shows the characteristic peaks at 2θ = 15.12° and 22.74°. In the DEC pattern, characteristic peaks disappeared, and new peaks emerged at 20.20°. The crystalline structure of EC was damaged, indicating that hydrogen bonds of the original EC were broken during modification.

Compared with EC, characteristic peaks of DEC disappeared and new peaks emerged at 20.20°, and the intensity of the diffraction peak decreased significantly. The hydroxyl groups on the glycosides of EC are substituted during the quaternization process, leading to breakage of hydrogen bonds of the original EC. At the same time, the introduction of quaternary ammonium groups disturbed the regularity of the entire molecular chain, destroying the crystalline regions in the molecular structure and increasing the amorphous region [29]. Sodium hydroxide solution treatment also contributed to the decrease in crystallization degree [30]. However, the spectrum of DEC still showed the characteristic peaks at 2θ = 20.20°, indicating that the crystal structure of cellulose was not completely destroyed during the modification process.

In addition to the increased intensity, the XRD patterns obtained from HEC and OEC had similar characteristics to DEC, indicating that the crystallinity of HEC and OEC were significantly affected by the difference in the alkyl chain length of modified agents. As the length of the alkyl chain increases, molecular segment movement became more difficult, and the quaternary ammonium salt molecules were less likely to penetrate the amorphous region and destroy the molecular structure of the cellulose units, thus resulting in higher crystallinity.

Table 2
The effect of the molar ratio on the *N*% and the degree of substitution

Sample	Molar ratio	*N*%	D_s
DEC	1.10	1.97	0.40
	1.20	2.10	0.45
	1.30	2.25	0.51
HEC	1.10	1.70	0.35
	1.20	1.83	0.40
	1.30	1.94	0.45
OEC	1.10	1.51	0.30
	1.20	1.67	0.36
	1.30	1.76	0.40

3.1.4. SEM

SEM photographs of EC, DEC, HEC and OEC were obtained at a magnification of 5000X as shown in Fig. 2. It can be clearly seen that the surface of EC is coarse and rough. After modification, the surface morphology changed significantly. DEC, HEC and OEC appear to have a smoother surface with a uniform wrinkled structure.

3.2. Adsorption performance of DEC, HEC and OEC

Effects of dosage on the adsorption performance of Acid Blue 93 are shown in Fig. 3. As for DEC, HEC and OEC, the dye removal deficiency followed the same pattern as the dosage increased from 0.2 to 1.4 g L^{-1}, and the trend of removal deficiency at other temperatures was similar. With the increase in Adsorbent dosage, the total number of active sites increased, resulting in an increase in the contact rate between the dye and the active sites. High adsorbent dosage promoted the removal of Acid Blue 93 dye. On the other hand, the adsorption capacity decreased rapidly as the adsorbent dosage increased. This decrease indicates that the adsorbent

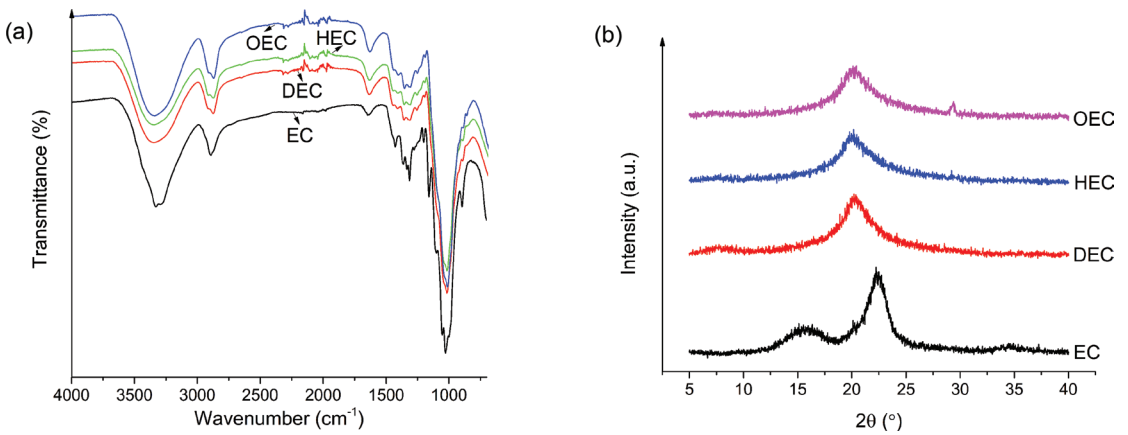

Fig. 1. FTIR (a) and XRD (b) spectra of EC, DEC, HEC and OEC.

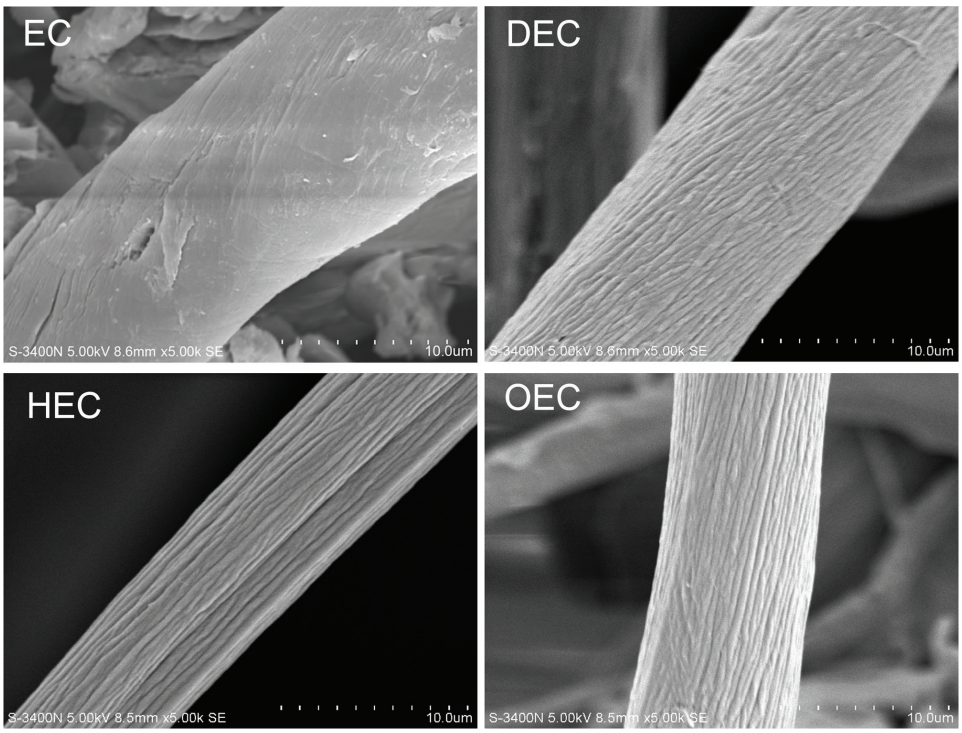

Fig. 2. SEM images of EC, DEC, HEC and OEC.

was not fully utilized and that a higher number of adsorption sites remained unoccupied with increased adsorbent dosage.

The effect of contact time and temperature on the adsorption performance of Acid Blue 93 dye on the DEC, HEC and OEC is shown in Fig. 3. It can be seen that, over a certain period of time, as the contact time increased, the adsorption capacities of Acid Blue 93 increased rapidly during the first 60 min, and then the numerical growth rate slowed down to reach an equilibrium; the adsorption capacities did not even change. Moreover, the adsorption capacities of Acid Blue 93 dye onto DEC, HEC and OEC increased with the increase in temperature. Raising the temperature favored the adsorption process.

The influence of the initial dye concentration on the adsorption performance of Acid Blue 93 dye onto DEC, HEC and OEC is shown in Fig. 3. When the dye concentrations were increased from 80 to 140 mg L^{-1}, the adsorption capacity of Acid Blue 93 dye onto DEC increased from 164.85 to 260.46 mg g^{-1}, 170.58 to 302.18 mg g^{-1} and 185.08 to 322.01 mg g^{-1} at 303.15, 313.15, and 323.15 K, respectively. As the initial concentration of the dye increased, there was a resulting increase in the concentration gradient. This is the driving force between the solution and the adsorbent, and the dye molecules are more easily combined with the adsorbent [14]. Therefore, the adsorption capacity increased with increasing initial dye concentration. The adsorption capacity showed the same trend with the effect of initial dye concentration for the adsorbent HEC and OEC.

3.3. Mechanisms of dye removal

The point of zero charge (pH_{PZC}) was measured by the previously described method [31]. The effect of pH on the adsorption of Acid Blue 93 onto DEC, HEC and OEC was also determined. The pH values were adjusted from 2 to 11 by adding a certain amount of NaOH or HCl solution. All the data used for the above analysis were the mean values from three replicate tests.

The pH value not only affects the surface charge properties, the functional groups, and the degree of ionization of the adsorbent in the bath, but also affects the structural properties of dye molecules. The pHpzc curves of the adsorbents DEC, HEC and OEC are shown in Fig. 4(a). It can be seen from the figure that the pHpzc of DEC, HEC and OEC was 7.23, 7.14 and 7.09, respectively. The effect of the pH of the aqueous solution on Acid Blue 93 adsorption onto adsorbent was investigated (Fig. 4(b)). The adsorption capacity increased as the pH rose from 2 to 11. A higher positive charge developed on its surface at pH values below pHpzc; this charge decreased at pH values above pHpzc [32]. In theory, the adsorption capacity should reach a maximum at pHpzc if the surface charge properties of the adsorbent is the only influencing factor for dye adsorption. Since the adsorption did not reach a peak at pHpzc, other factors inevitably affect the adsorption process. For the upon dye adsorption, at lower pH, $–SO_3^-$ groups in the dye molecule are protonated to $–SO_3H$ groups, resulting in the decrease of the electrostatic attraction between $–SO_3^-$ and $–NH_3^+$ groups of DEC, HEC and OEC. Upon an increase in pH values, the amount of $–SO_3^-$ groups increased, thereby increasing the adsorption capacity. Under alkaline conditions, the competition of OH^- ions will reduce the adsorption capacity, which is weaker than electrostatic attraction between the $–SO_3^-$ and $–NH_3^+$ groups [30]. Therefore, the adsorption capacities increased as the pH values increased.

Moreover, the adsorption capacities of Acid Blue 93 onto DEC, HEC and OEC were followed in the order

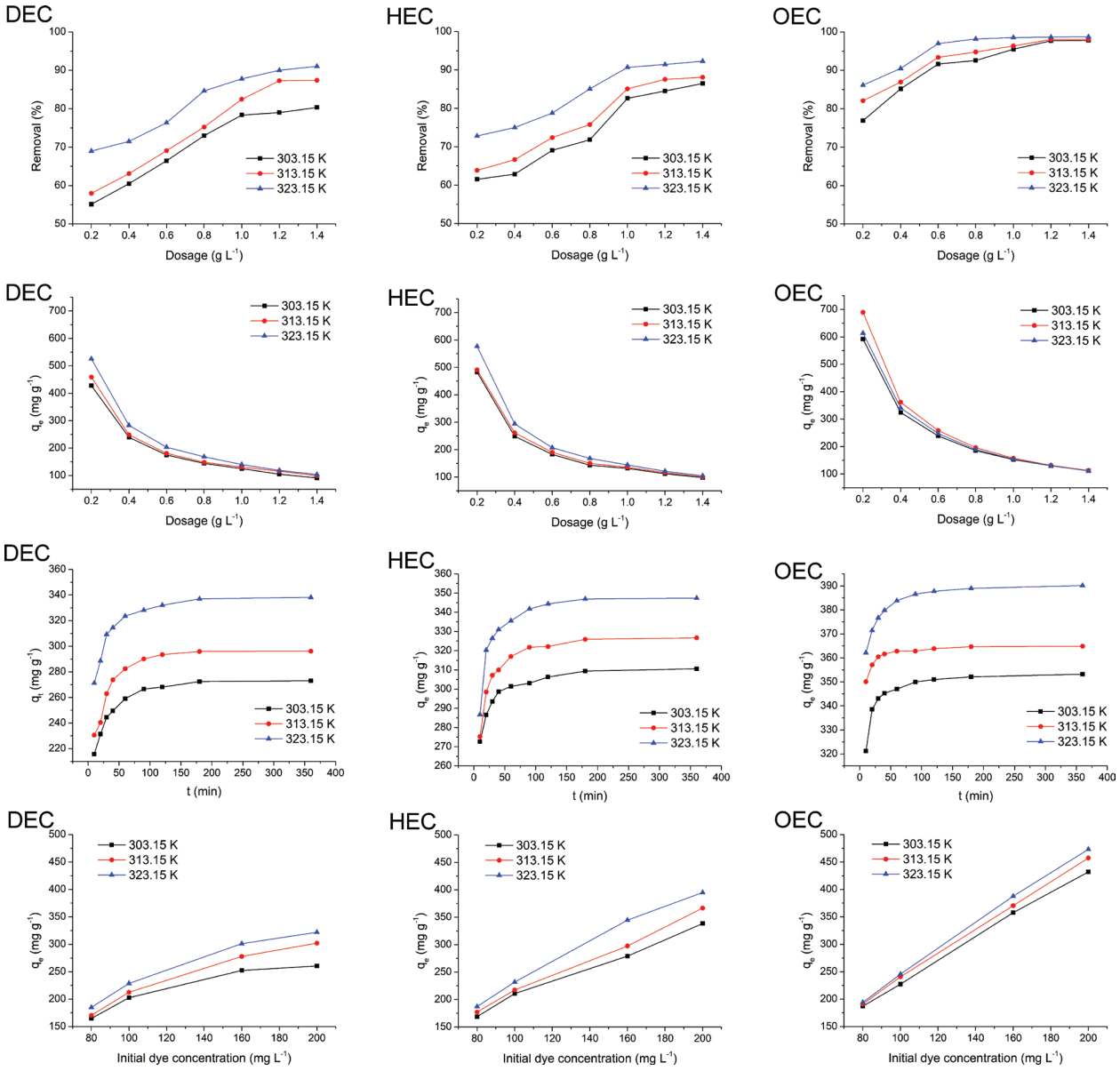

Fig. 3. Effects of dosage, contact time and initial dye concentration on the adsorption performance of DEC, HEC and OEC.

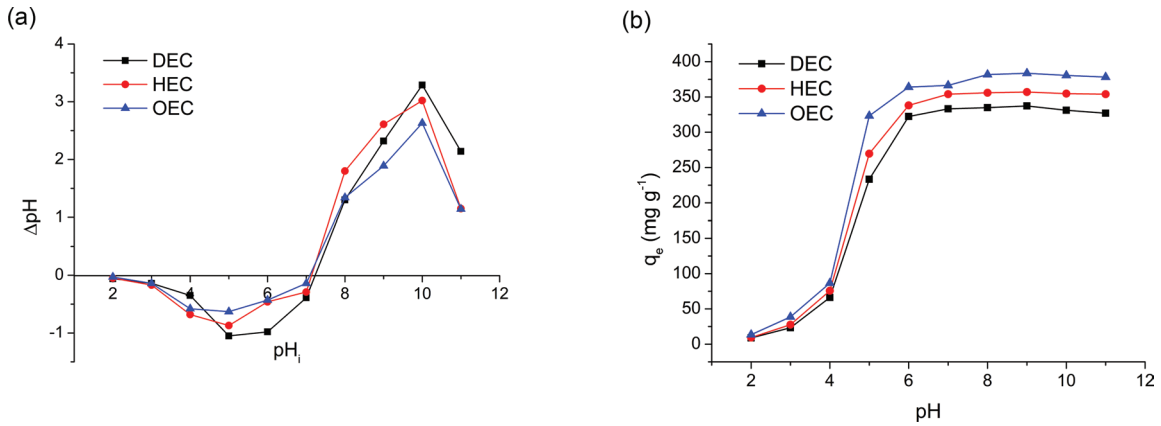

Fig. 4. (a) Point of zero charge of DEC, HEC and OEC, (b) Effects of pH on Acid Blue 93 adsorption onto DEC, HEC and OEC.

OEC > HEC > DEC. The adsorption capacity increased with an increase in the alkyl chain length of the cationized *Eucalyptus* wood chips cellulose. As the length of the alkyl chain increases, the hydrophobicity of the adsorbent increases, and the hydrophobic environment causes the dye to be close to the surface of the adsorbent, and the hydrogen bond is more easily formed, resulting in an increase in adsorption capacity. Moreover, the mutual repulsion between the ionic quaternary ammonium groups on the long-chain molecules makes the long-chain molecules more diffuse in water, resulting in a better coagulation performance of the adsorbent with a longer alkyl chain. The possible adsorption mechanism of Acid Blue 93 onto DEC, HEC and OEC is shown in Fig. 5.

3.4. Adsorption kinetics

Pseudo-first-order kinetics mainly describe the physical adsorption behavior that plays a dominant role in the adsorption process. Pseudo-second-order kinetics are often more suitable for describing adsorption processes where chemisorption plays a dominant role. The Elovich kinetic model is often used to describe the adsorption behavior of contaminants on heterogeneous solid adsorbents. The non-linear fitting results of the removal of Acid Blue 93 by DEC, HEC and OEC at different temperatures are shown in Fig. 6, and the fitting parameters are shown in Table 3.

The correlation R^2 values are often used to evaluate the correlation coefficients, so as to determine the adsorption kinetics during the adsorption process. In this experiment, at the different temperatures employed (303.15, 308.15, and 313.15 K), the R^2 value of the pseudo-second-order kinetics was higher than that of pseudo-first-order kinetics models. A higher R^2 coefficient value reveals that it would be more appropriate to use pseudo-second-order kinetics to analyze the purification behavior of Acid Blue 93 onto DEC, HEC and OEC. In addition, the closer adsorption capacity ($q_{e.cal}$) obtained by the pseudo-second-order kinetics and the experimentally measured adsorption capacity ($q_{e.exp}$) also supports

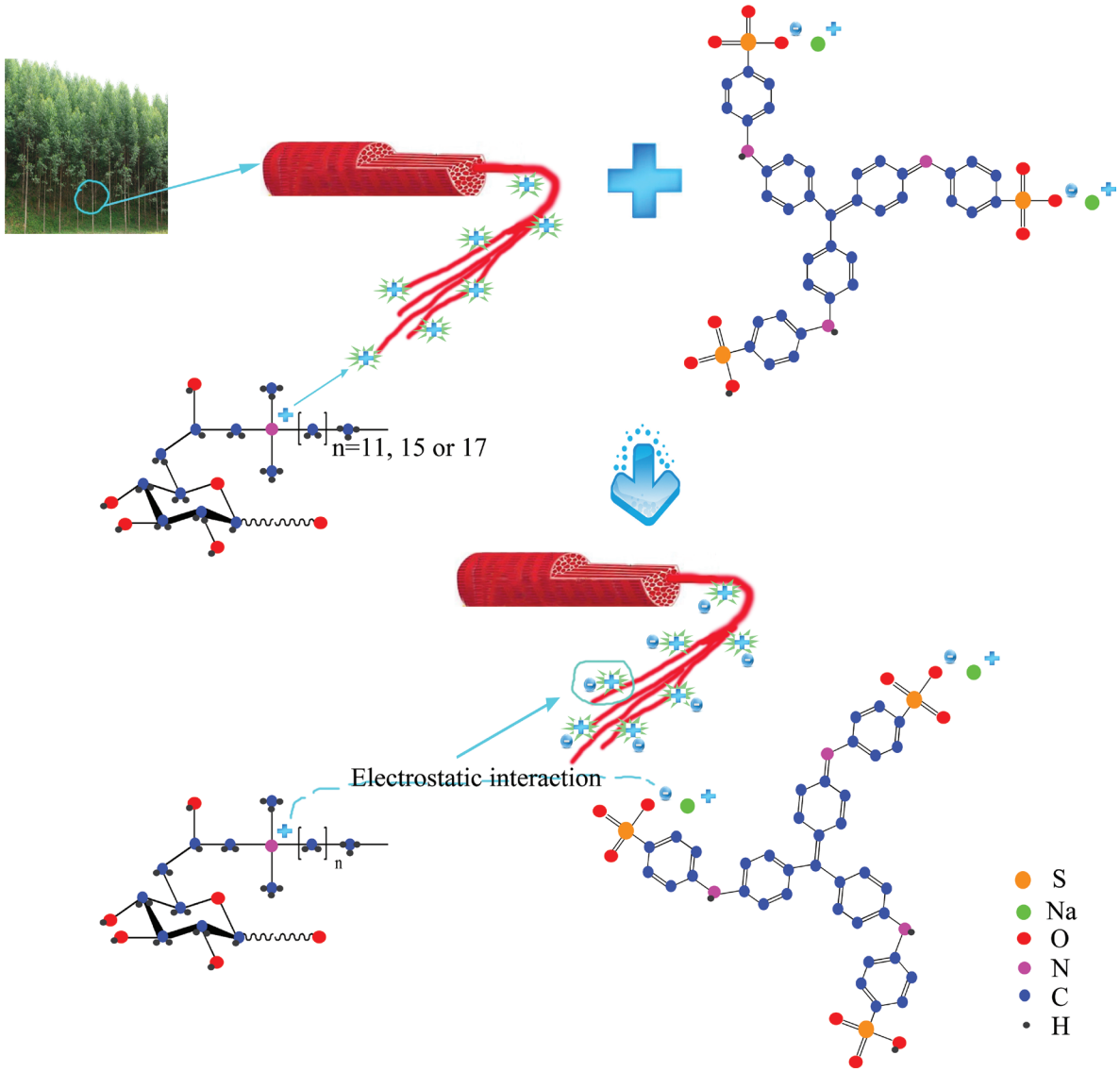

Fig. 5. The possible adsorption mechanism of Acid Blue 93 onto DEC, HEC and OEC.

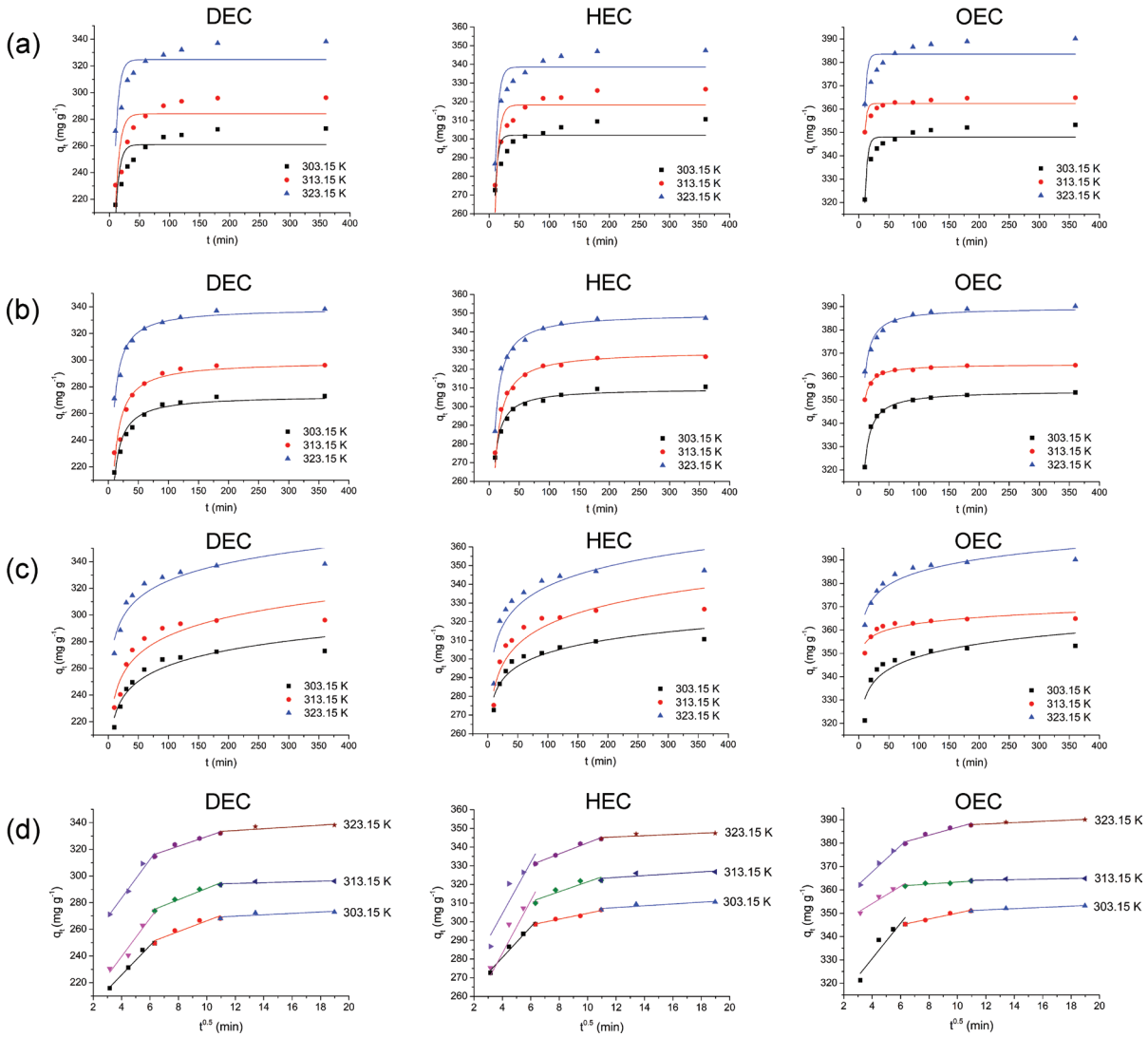

Fig. 6. Kinetic adsorption plots of Acid Blue 93 onto DEC, HEC and OEC: Pseudo-first-order (a), Pseudo-second-order (b), Elovich (c) and the intra-particle diffusion (d).

Table 3
Kinetics parameters on the adsorption of Acid Blue 93 onto DEC, HEC and OEC

Dyes	Pseudo-first-order			Pseudo-second-order			Elovich			$q_{e,\exp}$
	k_1	$q_{e,\mathrm{cal}}$	R^2	K_2	$q_{e,\mathrm{cal}}$	R^2	α	β	R^2	
DEC										
303.15 K	0.068	260.98	0.6021	0.0012	273.48	0.9520	92.07	0.059	0.8996	273.03
313.15 K	0.061	284.00	0.5841	0.00094	298.89	0.9234	23.64	0.049	0.8543	296.14
323.15 K	0.070	324.64	0.6397	0.0011	338.82	0.9624	44.20	0.053	0.8736	338.17
HEC										
303.15 K	0.097	302.01	0.6377	0.0022	309.68	0.9749	73.74	0.098	0.8790	310.60
313.15 K	0.074	318.24	0.8422	0.0013	329.64	0.9918	15.56	0.065	0.7632	326.69
323.15 K	0.078	338.56	0.8197	0.0014	349.93	0.9888	66.80	0.066	0.7780	347.38
OEC										
303.15 K	0.11	347.98	0.7969	0.0028	353.98	0.9943	14.61	0.14	0.7598	353.20
313.15 K	0.15	362.38	0.7308	0.0063	365.28	0.9936	81.07	0.27	0.7552	364.86
323.15 K	0.12	383.49	0.5483	0.0031	389.47	0.9572	12.89	0.13	0.8866	390.13

the above conclusion. Therefore, the above analysis of our results shows that the pseudo-first-order kinetic model can better describe the adsorption behavior of Acid Blue 93 onto DEC, HEC and OEC compared with the first-order kinetic model. The purification of Acid Blue 93 by DEC, HEC and OEC may be a chemical process, however, the activated energy of Acid Blue 93 was 5.51, 10.62 and 23.24 kJ mol^{-1}, which are all lower than 40 kJ mol^{-1}, so the purification process belongs to physical adsorption [33]. Moreover, the non-linear fitting of Elovich model yielded a high R^2 coefficient of determination value which indicates that there may be non-uniformities on the surface of the solid adsorbent.

3.5. Adsorption isotherms

In order to more accurately analyze the process, the most commonly used isotherm models, namely the Langmuir, Freundlich, Temkin and Sips models, were used in this study to describe how dyes interact with DEC, HEC and OEC. Langmuir is often proposed under certain assumptions (uniform adsorbent surface, monolayer adsorption). In fact, the surface of the adsorbent is often not uniform, multilayer adsorption often occurs, and an interaction force may exist between the adsorbed substances. Therefore, analysis using the Langmuir model alone is incomplete. Compared with the Langmuir model, the Freundlich model can make up for its deficiencies and is suitable for the analysis of more complex adsorption mechanisms. The Tempkin model is based on the linear relationship between the heat of adsorption and the temperature, which can describe the adsorption mechanism well. The Sips model combines the characteristics of the Langmuir and Freundlich models to reveal the heterogeneity of the adsorbent surface. This is consistent with the Freundlich model when the dyes are at a low concentration and the Langmuir model when the dyes are at a high concentration. Based on the above discussion, the experiment uses the monomolecular Langmuir, multi-molecule Freundlich, Temkin, Sips models for nonlinear fitting to analyze the isothermal adsorption behavior. The related parameters of non-linear data processing are shown in Table 4.

A higher R^2 coefficient value reveals that the adsorption behavior of DEC, HEC and OEC for Acid Blue 93 is applicable to the Langmuir and Sips models. However, the more similar $q_{e.cal}$ and $q_{e.exp}$ values suggest that the Langmuir model is more suitable for the analysis of this isothermal adsorption behavior. Among them, the value of *K*a by Langmuir is less than 1, indicating that the occurrence of the adsorption process is favorable. In addition, the reversibility of the adsorption

Table 4
Isotherm parameters on the adsorption of Acid Blue 93 onto DEC, HEC and OEC

Isotherms	DEC			HEC			OEC		
	303.15 K	313.15 K	323.15 K	303.15 K	313.15 K	323.15 K	303.15 K	313.15 K	323.15 K
Langmuir model									
q_m	288.70	336.21	367.50	362.75	393.16	451.53	551.77	581.73	609.35
K_a	0.11	0.10	0.25	0.0059	0.0045	0.068	0.090	0.29	0.75
R^2	0.9417	0.9644	0.9612	0.9993	0.9997	0.9747	0.9847	0.9781	0.9593
R_L	0.050	0.055	0.11	0.68	0.75	0.16	0.066	0.022	0.0087
Freundlich model									
$1/n_f$	0.21	0.25	0.19	0.81	0.87	0.44	0.48	0.40	0.38
k_F	104.45	101.78	146.49	11.97	11.80	81.76	91.14	159.65	247.76
R^2	0.8644	0.9307	0.9156	0.9979	0.9990	0.9129	0.9913	0.9989	0.9178
Temkin model									
A_T	3.30	1.81	10.11	0.096	0.10	0.53	0.78	2.73	6.72
B	46.63	61.81	49.68	186.35	211.82	133.14	141.04	122.44	130.40
R^2	0.8910	0.9488	0.9343	0.9909	0.9888	0.9658	0.9813	0.9914	0.9513
Sips model									
q_m	258.24	299.25	313.30	992.14	403.98	360.57	473.34	564.60	658.62
K_s	0.0012	0.015	0.026	0.0062	0.0052	0.0035	0.070	0.11	0.80
$1/n$	2.97	1.91	2.33	1.07	1.06	1.12	0.65	0.50	1.08
R^2	0.9903	0.9440	0.9530	0.9989	0.9996	0.6688	0.9871	0.9999	0.9196
q_e	260.46	302.18	322.01	338.58	366.79	395.12	431.98	457.32	473.24

behavior can be further analyzed by the R_L value. When $R_L = 0$, the adsorption is an irreversible process; when $0 < R_L < 1$, it indicates that the adsorption process is favorable; when $R_L = 1$, the adsorption isotherm is linear; when $R_L > 1$, the adsorption process is unfavorable [11]. In this experiment, the R_L values of the adsorbents DEC, HEC and OEC for Acid Blue 93 adsorption were in the range of $0 < R_L < 1$, further illustrating that the adsorption process was favorable for adsorption.

3.6. Thermodynamic evaluation

Table 5 shows the thermodynamic parameters for adsorption of Acid Blue 93 onto DEC, HEC and OEC. The values of $\Delta G°$ are negative, and the increasing trend of the value is consistent with the increasing trend of temperature, revealing that the adsorption was spontaneous and is a feasible purification process. The values of $\Delta H°$ are all positive, indicating that the adsorption process was endothermic, so that raising the temperature favored the adsorption of Acid Blue 93 dyes onto DEC, HEC and OEC. The values of $\Delta S°$ are all positive, revealing the degree of high randomness for adsorption behavior. In addition, whether the process is best described by physical or chemical adsorption can be determined by analyzing the standard $\Delta H°$ value. When $\Delta H° < 20$ kJ mol^{-1}, physical adsorption plays an important role in the form of van der Waals interactions. When 20 kJ mol^{-1} $< \Delta H° <$ 80 kJ mol^{-1}, the electrostatic interaction plays an important role in the physical purification process [34]. When $\Delta H° > 80$ kJ mol^{-1}, the adsorption process is mainly a result of chemical adsorption. In this experiment, the $\Delta H°$ values of DEC, HEC and OEC for the purification of Acid Blue 93 were all less than 80 kJ mol^{-1}, indicating that physical adsorption was the major contributor to the purification process; this is consistent with the conclusion of the kinetic analysis.

Table 5
Thermodynamic parameters for adsorption of Acid Blue 93 onto DEC, HEC and OEC

Dyes	$\Delta H°$ (kJ mol^{-1})	$\Delta S°$ (J mol^{-1} K^{-1})	$\Delta G°$ (kJ mol^{-1})		
			303.15 K	313.15 K	323.15 K
DEC	19.92	74.44	−2.58	−3.44	−3.80
HEC	17.49	79.72	−6.70	−7.18	−7.79
OEC	64.04	234.11	−7.05	−8.73	−11.02

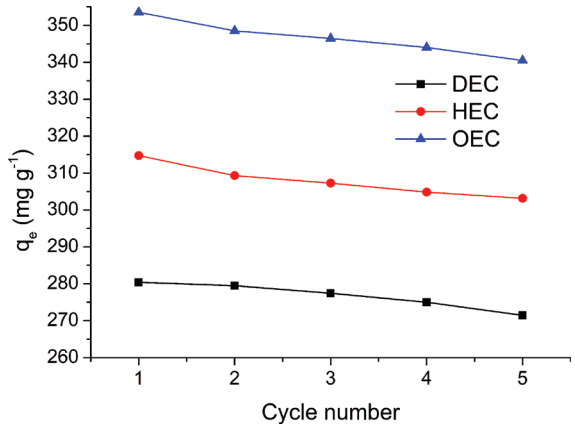

Fig. 7. The reusability of DEC, HEC, and OEC for acid blue 93 adsorption.

3.7. Adsorbent reusability

From the practical point of view, the reusability experiments are likely to be a key factor in evaluating the practical application of the adsorbents. The adsorption-desorption cycle was repeated five times and the results are shown in Fig. 7. The adsorption capacity decreased with an increase in the number of cycles. However, the adsorption capacities of DEC, HEC, and OEC for Acid Blue 93 decreased slowly with increasing cycle number, remaining at a high adsorption capacity even at the fifth cycle. Thus, the DEC, HEC, and OEC have a good reusability and high adsorption performance for the removal of Acid Blue 93 dye.

4. Conclusions

Cationized *Eucalyptus* wood chips cellulose (DEC, HEC and OEC) was prepared via grafting with quaternary ammonium group using *N,N*-dimethyl-1-dodecylamine, *N,N*-dimethyl-1-hexadecylamine or *N,N*-dimethyl-1-octadecylamine as modification agents on EC microstructure. Structural and morphological characterizations were performed using FTIR, XRD and SEM analysis. The characterization results showed that the molecular structure and morphology of EC were modified by the process and that the quaternary ammonium group was successfully grafted onto the RHC molecular structure. DEC, HEC and OEC with the same degree of substitution were selected as the adsorbents for the adsorption of Acid Blue 93 dye to evaluate the adsorption performance and adsorption mechanism for dyes of cationized cellulose with different molecular structures. The adsorption process was well described by pseudo-second-order and Langmuir models. The maximum adsorption capacities of Langmuir for Acid Blue 93 onto the DEC, HEC and OEC were 288.70, 362.75 and 551.77 mg g^{-1} at 303.15 K, respectively. The adsorption capacities increased with the increasing alkyl chain lengths of DEC, HEC and OEC. The adsorbents were shown to have a good reusability and high adsorption performance for dye removal. Fitting results for non-linear kinetics and isotherms showed that pseudo-second-order and Langmuir models were most suitable for describing the characteristics of Acid Blue 93 adsorption onto DEC, HEC and OEC. The adsorption process is a spontaneous and feasible purification process that is made more conducive at higher temperatures.

Acknowledgements

This work was supported by the Young and middle-aged teachers' basic ability improvement project of the Guangxi universities (2018KY0033) and Natural Science Foundation of Guangxi (2018GXNSFBA138025).

References

[1] A.M. Das, A.A. Ali, M.P. Hazarika, Synthesis and characterization of cellulose acetate from rice husk: eco-friendly condition, Carbohydr. Polym., 112 (2014) 342–349.

[2] A.L. Squissato, A.F. Lima, E.S. Almeida, D. Pasquini, E.M. Richter, R.A. Munoz, Eucalyptus pulp as an adsorbent for metal removal from biodiesel, Ind. Crop. Prod., 95 (2017) 1–5.
[3] Y.M. Chen, J.Q. Wan, X.L. Zhang, Y.W. Ma, Y. Wang, Effect of beating on recycled properties of unbleached eucalyptus cellulose fiber, Carbohydr. Polym., 87(2012) 730–736.
[4] G.H.D. Tonoli, E.M. Teixeira, A.C. Corrêa, J.M. Marconcini, L.A. Caixeta, M.A. Pereira-da-Silva, L.H.C. Mattoso, Cellulose micro/nanofibres from eucalyptus kraft pulp: preparation and properties, Carbohydr. Polym., 89 (2012) 80–88.
[5] S. Arola, J.M. Malho, P. Laaksonen, M. Lille, M.B. Linder, The role of hemicellulose in nanofibrillated cellulose networks, Soft Matter, 9 (2013) 1319–1326.
[6] J.K. Xu, H.J. Hou, B.C. Liu, J.P. Hu, The integration of different pretreatments and ionic liquid processing of eucalyptus: hemicellulosic products and regenerated cellulose fibers, Ind. Crop. Prod., 101 (2017) 11–20.
[7] W.X. Wang, G.H. Huang, C.J. An, S. Zhao, X.J. Chen, P. Zhang, Adsorption of anionic azo dyes from aqueous solution on cationic gemini surfactant-modified flax shives: synchrotron infrared, optimization and modeling studies, J. Clean. Prod., 172 (2018) 1986–1997.
[8] H. Kono, Cationic flocculants derived from native cellulose: preparation, biodegradability, and removal of dyes in aqueous solution, Resour. Effic. Technol., 3 (2017) 55–63.
[9] A. Khatri, M.H. Peerzada, M. Mohsin, M. White, A review on developments in dyeing cotton fabrics with reactive dyes for reducing effluent pollution, J. Clean. Prod., 87 (2015) 50–57.
[10] H. Kono, K. Ogasawara, R. Kusumoto, K. Oshima, H. Hashimoto, Y. Shimizu, Cationic cellulose hydrogels cross-linked by poly (ethylene glycol): preparation, molecular dynamics, and adsorption of anionic dyes, Carbohydr. Polym., 152 (2016) 170–180.
[11] Y. Safa, H.N. Bhatti, Kinetic and thermodynamic modeling for the removal of direct red-31 and direct orange-26 dyes from aqueous solutions by rice husk, Desalination, 272 (2011) 313–322.
[12] I. Urruzola, L. Serrano, R. Llano-Ponte, M.Á. de Andrés, J. Labidi, Obtaining of eucalyptus microfibrils for adsorption of aromatic compounds in aqueous solution, Chem. Eng. J., 229 (2013) 42–49.
[13] X.H. Zhu, Y.B. Wen, D. Cheng, C.M. Li, X.Y. An, Y.H. Ni, Cationic amphiphilic microfibrillated cellulose (MFC) for potential use for bile acid sorption, Carbohydr. Polym., 132 (2015) 598–605.
[14] M.T. Yagub, T.K. Sen, S. Afroze, H.M. Ang, Dye and its removal from aqueous solution by adsorption: a review, Adv. Colloid Interface Sci., 209 (2014) 172–184.
[15] H. Sehaqui, U.P. de Larraya, P. Tingaut, T. Zimmermann, Humic acid adsorption onto cationic cellulose nanofibers for bioinspired removal of copper (II) and a positively charged dye, Soft Matter, 11 (2015) 5294–5300.
[16] X.Y. Zhang, J. Tan, X.H. Wei, L.J. Wang, Removal of remazol turquoise blue G-133 from aqueous solution using modified waste newspaper fiber, Carbohydr. Polym., 92 (2013) 1497–1502.
[17] A. Hashem, R.M. El-Shishtawy, Preparation and characterization of cationized cellulose for the removal of anionic dyes, Adsorpt. Sci. Technol., 19 (2011) 197–210.
[18] Y. Qi, J. Li, L.J. Wang, Removal of remazol turquoise blue G-133 from aqueous medium using functionalized cellulose from recycled newspaper fiber, Ind. Crop. Prod., 50 (2013) 15–22.
[19] B.L. Zhao, Y. Shang, W. Xiao, C.C. Dou, R.P. Han, Adsorption of congo red from solution using cationic surfactant modified wheat straw in column model, J. Environ. Chem. Eng., 2 (2014) 40–45.
[20] P.J. Quinlan, A. Tanvir, K.C. Tam, Application of the central composite design to study the flocculation of an anionic azo dye using quaternized cellulose nanofibrils, Carbohydr. Polym., 133 (2015) 80–89.
[21] Y. Chen, X.H. Chen, Y.W. Liu, Z.N. Yang, Z. Zhang, Evaluation of physical and chemical adsorption using electrochemical noise technique for methylene blue on mild steel, J. Chem. Thermodyn. 126 (2018) 147–159.
[22] M. Maheshwari, R.K. Vyas, M. Sharma, Kinetics, equilibrium and thermodynamics of ciprofloxacin hydrochloride removal by adsorption on coal fly ash and activated alumina, Desal. Wat. Treat., 51 (2013) 7241–7254.
[23] D.Y. Hu, L.J. Wang, Adsorption of amoxicillin onto quaternized cellulose from flax noil: kinetic, equilibrium and thermodynamic study, J. Taiwan Inst. Chem. Eng., 64 (2016) 227–234.
[24] C.J. An, S.Q. Yang, G.H. Huang, S. Zhao, P. Zhang, Y. Yao, Removal of sulfonated humic acid from aqueous phase by modified coal fly ash waste: equilibrium and kinetic adsorption studies, Fuel, 165 (2016) 264–271.
[25] Y.B. Song, J. Zhang, W.P. Gan, J.P. Zhou, L.N. Zhang, Flocculation properties and antimicrobial activities of quaternized celluloses synthesized in NaOH/urea aqueous solution, Ind. Eng. Chem. Res., 49 (2009) 1242–1246.
[26] M. Zaman, H.N. Xiao, F. Chibante, Y.H. Ni, Synthesis and characterization of cationically modified nanocrystalline cellulose, Carbohydr. Polym., 89 (2012) 163–170.
[27] H. Kono, R. Kusumoto, Removal of anionic dyes in aqueous solution by flocculation with cellulose ampholytes, J. Water Process Eng., 7 (2015) 83–93.
[28] P.J. Quinlan, A. Tanvir, K.C. Tam, Application of the central composite design to study the flocculation of an anionic azo dye using quaternized cellulose nanofibrils, Carbohydr. Polym., 133 (2015) 80–89.
[29] H. Liimatainen, T. Suopajärvi, J. Sirviö, O. Hormi, J. Niinimäki, Fabrication of cationic cellulosic nanofibrils through aqueous quaternization pretreatment and their use in colloid aggregation, Carbohydr. Polym., 103 (2014) 187–192.
[30] F.L. Zhang, Z.Q. Pang, C.H. Dong, Z. Liu, Preparing cationic cotton linter cellulose with high substitution degree by ultrasonic treatment, Carbohydr. Polym., 132 (2015) 214–220.
[31] H.R. Pouretedal, N. Sadegh, Effective removal of amoxicillin, cephalexin, tetracycline and penicillin G from aqueous solutions using activated carbon nanoparticles prepared from vine wood, J. Water Process Eng., 1 (2014) 64–73.
[32] S. Chowdhury, R. Mishra, P. Saha, P. Kushwaha, Adsorption thermodynamics, kinetics and isosteric heat of adsorption of malachite green onto chemically modified rice husk, Desalination, 265 (2011) 159–168.
[33] W. Konicki, D. Sibera, E. Mijowska, Z. Lendzion-Bielun, U. Narkiewicz, Equilibrium and kinetic studies on acid dye Acid Red 88 adsorption by magnetic $ZnFe_2O_4$ spinel ferrite nanoparticles, J. Colloid Interface Sci., 398 (2013) 152–160.
[34] M.S. Maleki, O. Moradi, S. Tahmasebi, Adsorption of albumin by gold nanoparticles: equilibrium and thermodynamics studies, Arab. J. Chem., 10 (2017) S491–S502.